Articles

The Activating Transcription Factor Region within the E2A Promoter Exists in a Novel Conformation†

Katherine L. B. Borden*

Laboratory of Molecular Structure, The National Institute for Medical Research, The Ridgeway, Mill Hill, London NW7 1AA, U.K.

Received September 3, 1992; Revised Manuscript Received March 10, 1993

ABSTRACT: The ATF (activating transcription factor) binding site within the E2A promoter region of adenovirus is shown to exist in a novel conformation *in vitro* via nuclear magnetic resonance methods. This novel conformation may be important to the protein DNA recognition process. This conformation has characteristics of both A- and B-form DNA. From circular dichroism and through-space-based NMR experiments, it is clear that the overall helical structure is B-like. However, the ^1H–^1H coupling constant information indicates that most of the sugar puckers of the individual nucleotides are in the C3′-endo/C4′-exo range which is more characteristic of A-form DNA. The sugar conformation can also be described as a mixture of two states, C3′-endo and C2′-endo, where many of the sugars exist mainly in the C3′-endo state. These data show that the conformation of the sugar puckers does not determine the nature of the overall base stacking on the DNA. Helical parameters were calculated from NOE build-up curves for half of the dinucleotide pairs. Severe spectral overlap on the nuclear Overhauser based spectra prevented determination of the helical parameters for all of the dinucleotide base-pairs. Energy minimization and molecular dynamic simulation methods using the sugar pucker and glycosidic torsion angles determined from the NMR data as constraints were carried out in order to demonstrate that such a conformation was energetically favorable.

The structures of protein DNA (and RNA) complexes have been studied in order to attain a better understanding of the recognition processes central to cellular control events [for reviews, see Steitz (1991) and Freemont et al. (1991)]. The structures of many DNA and RNA sequences have been determined in the absence of protein. Therefore, one can ascertain if there are any structural features specific to certain types of oligonucleotide sequences which may be involved in the specificity of the protein nucleic acid recognition process.

Recently, a new family of eukaryotic transcription factors, the ATF (activating transcription factor) family, has been found in embryonic carcinoma cells (Tassios & LaThangue, 1990). A number of ATF binding sites have been found in systems other than the embryonic carcinoma cells, including the E2A and E4 promoters of adenovirus and the promoter for human vasoactive intestinal peptide (Hai et al., 1989; Tassios & LaThangue, 1990). The ATF proteins contain a leucine heptad repeat region (putative dimerization domain) adjacent to a basic region (putative DNA binding domain) which is similar to that of the c-jun/AP-1 proteins (Hai et al., 1989). This paper reports the results of an investigation of the structure of the ATF binding site from adenovirus.

Several biologically important oligonucleotide structures have been determined both in solution by NMR in conjunction with circular dichroism methods and in the solid state by X-ray crystallography and X-ray fiber diffraction. The two most frequently occurring conformers of DNA are known as the A-form and the B-form. This nomenclature arose from the pattern of spots observed in X-ray fiber diffraction experiments. Both A- and B-DNA are right-handed double-stranded helices: these conformers have different values for intranucleotide and helical parameters. For instance, B-DNA typically has a glycosidic torsion angle of roughly −110°, and sugar puckers are near C2′-endo: in A-DNA, the glycosidic torsion angles are about −150°, and the sugar puckers are near C3′-endo (Saenger, 1984). These differences in nucleotide conformation may necessitate the differences observed in the helical parameters.

Different conditions seem to favor one form of DNA over another. In general, B-like conformers have been identified in solution and both A-like and B-like conformers are found in crystals. The appearance of A-like conformers may be a result of the dehydrating conditions used to obtain crystals. This notion is supported by experiments done by Aboula-ela et al. (1988), who have shown via NMR and circular dichroism methods that the TFIIIA binding site is B-form in solution whereas earlier crystal analysis had indicated that the identical oligonucleotide was in the A-form (McCall et al., 1986). However, the work of Fairall et al. (1989) using circular dichroism suggests that in solution the TFIIIA binding site exists in an intermediate state between A and B. There have been some suggestions that there is actually a continuum of structures between the A- and B-forms (Lauble et al., 1988). The problem with such a theory is that the titration curves monitoring the interconversion of the A- and B-forms are sigmoidal, suggesting a strongly cooperative transition (Saenger, 1984).

In general, these reports suggest that DNA probably does not adopt strictly A- or B-forms. It is clear also that the

† This work was supported by the Medical Research Council of the U.K.

* Address correspondence to this author. Telephone: 081-959-3666. Fax: 081-906-4477. Telex: 922 666 (MRCNAT G).

0006-2960/93/0432-6506$04.00/0

individual nucleotide conformation does not define the helix type. For instance, in DNA/RNA hybrids, the overall helix conformation is A-like, but the DNA has C2′-endo sugar conformations and RNA has C3′-endo sugar conformations (Saenger, 1984; Chou et al., 1989). This also indicates that the helices themselves must be flexible to incorporate either sugar conformation because of the marked effect of sugar conformations on the phosphodiester backbone.

The studies of purine–purine mismatched base-pairs show that the B-helix can tolerate local structures which are not B-like but still retain the overall B-like character of the helix. This has been observed in A·G mismatched sequences where the glycosidic torsion angles are syn and anti at the mismatch site; however, this creates only a local lesion, and the remainder of the helix retains its B character (Gao & Patel, 1988; Lane et al., 1991; Carbonnaux et al., 1991). Large alterations in the phosphodiester backbone can also be tolerated as seen by large bulges in the backbone of a G·G mismatch (Borden et al., 1992) and in the backbone of a tandem GA mismatch (Li et al., 1991). These mismataches caused only a deviation from B-form DNA at the lesion site and base-pairs directly adjacent to it whereas the rest of the molecule retained its B-like conformation.

The solution conformations have been determined by NMR for many genetic control elements: trp operator, lac promoter, Pribnow box, *Eco*RI restriction site, etc. [see review by Lane (1989) and van de Ven and Hilbers (1988)]. The nucleotide conformation in these cases indicates anti-glycosidic torsion angles and sugar puckers which are 70–95% fraction south for nonterminal sugars (Rinkel et al., 1987; Bax & Lerner, 1988; Lane & Forster, 1989; Lane, 1989, 1991; Schmitz et al., 1990; van Wijk et al., 1992). No cases of B-like helices containing sugar puckers existing mainly in the north conformation have thus far been reported. Most DNA helices have an overall B-like form although there are local sequence-dependent changes. This indicates that a variety of sequences can be introduced into B-like forms with a modest adjustment of local parameters.

The study of the ATF binding site within the E2A promoter of adenovirus again shows the inherent flexibility of B-DNA. The oligonucleotide d(CCGCGTCTTC)·d(GAAGACGCGG) is studied by NMR and circular dichroism methods. This report demonstrates that one can incorporate sugar puckers in the range of C3′-endo/C4′-exo/O1′-endo into a B-form helix.

EXPERIMENTAL PROCEDURES

Synthesis and Purification of Oligonucleotides. The decamers d(CCGCGTCTTC) and d(GAAGACGCGG) were prepared on an Applied Biosystems synthesizer using phosphoramidite chemistry and purified by serial reverse-phase (C8) and ion-exchange FPLC as described previously (Leonard et al., 1990). The sample was lyophilized, and the two strands of DNA were dissolved in 1 mL of 10 mM sodium phosphate, 100 mM KCl, and 0.5 mM EDTA at pH 7.5. The A_{260} was measured for each strand so that they could be mixed in equal concentrations and thus maximize the yield of duplex DNA. The sample was annealed by incubation in a water bath at 80 °C for 5 min and then allowed to cool slowly. Then, native 20% acrylamide gels were run in the presence of ethidium bromide so that one could visualize the DNA under UV light and thereby ensure that there was no other species contaminating the sample. The final sample concentration was approximately 2 mM strands, pD* 7.2 (uncorrected for the isotope effect), and the final salt concentration was 20 mM sodium phosphate, 200 mM KCl, and 1 mM EDTA.

For experiments carried out in ^2H_2O, samples were lyophilized and then redissolved in 99.96% ^2H_2O from Aldrich. 4,4-Dimethylsilapentane-1-sulfonate (DSS, 0.1 mM) was used as an internal ^1H chemical shift reference.

Circular Dichroism (CD).[1] CD spectra were recorded on a JASCO Model J-600 spectropolarimeter at ambient temperature. The average of three scans was taken over the wavelength range of 330–205 nm and the buffer contribution was subtracted. The buffer used was the same as that used in the NMR studies. The sample concentration was 76 μM, and the cell path length was 0.2 mm. The resulting intensities were normalized to the duplex concentration and are reported in molar ellipticity.

NMR Spectroscopy. ^1H NMR spectra were collected in ^2H_2O at 11.7 T on a Bruker AM spectrometer and in ^1H_2O at 14.1 T on a Varian Unity spectrometer at 20 °C. One-dimensional-driven truncated NOEs in ^2H_2O were collected at 9.4 T on a Bruker AM spectrometer using the method of Wagner and Wuthrich (1979) at 20 °C. The acquisition time was 1.82 s. Irradiation times were varied from 50 to 600 ms with eight time points collected in total. The experiment was carried out twice. Rotational correlation times were determined from the cross-relaxation constant, σ, for the C(H5–H6) vector as previously described (Lane et al., 1986; Borden et al., 1992).

Phase-sensitive NOESY spectra were recorded in ^2H_2O at 50-, 100-, 150-, 200-, and 300-ms mixing times using time-proportional phase incrementation (Marion & Wuthrich, 1983). A total of 512 t_1 increments of 2048 data points were collected with an acquisition time of 170 ms in t_2 and 50 ms in t_1 and a 2-s recycle delay. Sine-modulated data were recorded by proper adjustment of the receiver phase and dead time to produce a flat base-plane (Frenkiel et al., 1990). Free induction decays were zero-filled to 2048 in $F1$ and 8192 in $F2$ and then Fourier-transform-apodized with a $\pi/3$-shifted sine-bell in both dimensions.

A NOESY spectrum in ^1H_2O was recorded at 8 °C at 11.7 T with a 200-ms mixing time and an acquisition period of 86 ms in t_2. The intense solvent signal was suppressed by presaturation. Under these conditions, the rate of exchange of nonterminal imino protons is sufficiently slow as to enable detection (Rajagopal et al., 1988). The data were processed as above.

A DQF-COSY spectrum with high digital resolution was recorded at 14.1 T using the method of States et al. (1982). A total of 600 t_1 increments of 8192 data points were collected. The acquisition time was 683 ms in t_2 and 50 ms in t_1. A high digital resolution TOCSY was also recorded at 14.1 T using MLEV17 (Bax & Davis, 1985) to produce isotropic mixing. A total of 512 t_1 increments of 4096 data points were collected. The acquisition time was 341 ms in t_2 and 43 ms in t_1. The spin-lock field strength was 8.3 kHz, and the mixing time was 50 ms. The free induction decays were zero-filled once in t_2 and twice in t_1. The spectrum was Fourier-transform-apodized with shifted Gaussian functions with 0.185-s width and a 0.005-s shift in t_2 and with 0.005-s width and shift in t_1.

ROESY spectra were recorded in ^2H_2O at 75-, 100-, and 200-ms mixing times at 9.4 T. Isotropic mixing was produced using the method of Bauer et al. (1990) and Bothner-By et al. (1984). The spin-lock field strength was 2.1 kHz. The acquisition time was 256 ms in t_2 and 50 ms in t_1.

[1] Abbreviations: CD, circular dichroism; NOE, nuclear Overhauser enhancement; NOESY, two-dimensional nuclear Overhauser enhancement spectroscopy; TOCSY, total correlation spectroscopy; DQF-COSY, double-quantum-filtered correlated spectroscopy.

One-dimensional NMR spectra were collected in ^1H_2O at 293 K using the $1\bar{3}3\bar{1}$ composite pulse for excitation (Hore, 1983) for assignment of the imino protons. Truncated NOEs were measured by irradiation of the imino protons for 50–1000 ms, and the acquisition period was typically 2 s.

NMR Data Analysis. NOESY cross-peak volumes were determined and normalized as described previously where the widths at half-height of cross sections parallel to *F*1 and *F*2 were multiplied together and the average peak height from the two cross-sections was used (Chary et al., 1988; Lane et al., 1990). The volumes were normalized to the volume of a single proton at zero mixing time. The value at zero mixing time was obtained by multiplying the volume of a diagonal peak by $\exp(R_1 t_m)$ where R_1 is the selective spin–lattice relaxation rate constant and t_m is the NOESY mixing time. R_1 is obtained independently from a selective saturation recovery experiment (Mirau, 1988). R_1's were determined for C16H6, A12H8, and A13/A15H8. These were the only resonances which were sufficiently well resolved. The volume at zero mixing time was calculated for the diagonal peaks of C16H6, A12H8, and A13/A15H8 in ^2H_2O. The average of the values for A12H8 and A13/A15H8 was calculated to normalize the volumes of cross-peaks of the purines, and the C16H6 value was used to normalize the volumes of the cross-peaks of the pyrimidines. Note that the use of the short recycle delay should not result in serious underestimation of the NOE intensities because of the method used for normalization. Since the cross-peak volumes are normalized to the volumes of the diagonal peaks from the same data set, any error in the intensities due to saturation should be minimized (also see below). Kim and Reid (1992) have shown empirically that using values of recycle delays only slightly larger than the values of the T_1's did not cause any significant error in subsequent intensity measurements.

Sugar puckers were determined from coupling constants as described by Rinkel and Altona (1987). Glycosidic torsion angles and helical parameters were determined from NOE time courses by using NUCFIT (Lane, 1990). For all data analysis using NUCFIT, the sugar pucker amplitude was fixed at 40° since by NMR this variable is not well determined (van de Ven & Hilbers, 1988). Helical parameters were also fit with the NUCFIT program. Any saturation due to an insufficiently long relaxation delay is accounted for in the NUCFIT program as the recycle delay is used as input (Lane, 1990). Subsequently, the program simulates the NMR data at the given recycle delay. Calculations using NUCFIT were carried out on a Macintosh LC.

Energy Minimization and Molecular Dynamics. Calculations were carried out on an Iris Indigo Elan Silicon Graphics system using Quanta 3.2. Experimental constraints were included as dihedral and torsion angles derived from pseudorotation and glycosidic torsion angles. The pseudorotation angles were converted into the dihedral angle δ by the method of Altona and Sundaralingam (1972). Calculations were done using the CHARMm force field *in vacuo* with the electrostatics component of the potential turned off.

Certain distances and torsion/dihedral angles were used as constraints. The C1′ (strand 1) to C1′ (strand 2) distance was set to 1.03 ± 0.03 nm, and the heavy atoms involved in imino base-pairing were set to 0.295 ± 0.02 nm which is typical for Watson and Crick base-pairs (Saenger, 1984). The sugar puckering and glycosidic torsion angles were determined for each nucleotide from the NMR data.

The protocol used for structure refinement consists of (i) 200 steps of conjugate gradient minimization to remove bad contacts, (ii) molecular dynamics with heating to 300 K during 1 ps (1.0-fs time step), and (iii) 10-ps dynamics (1.0-fs time step) with coupling to a heat bath at 300 K. The NMR constraints were weighted 25–50 times more heavily than the energy terms.

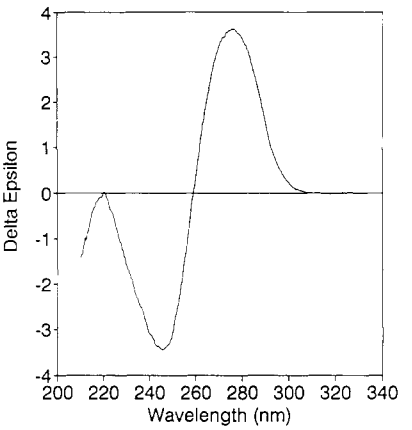

FIGURE 1: Circular dichroism spectrum of the ATF binding site within the E2A promoter of adenovirus. Buffer conditions (200 mM KCl, 20 mM sodium phosphate, and 1.0 mM EDTA) are the same as used in the NMR experiments. The sample concentration was 76 μM. See Experimental Procedures for details.

RESULTS AND DISCUSSION

Circular Dichroism. The CD spectrum of nucleic acids provides one with a global overview of the nature of the base stacking within the helix. A- and B-DNA have characteristic stacking patterns and therefore characteristic CD profiles (Ivanov et al., 1974; Saenger, 1984). Figure 1 shows the CD spectrum of the 10-mer. The maximum occurs at 275 nm and the miniumum at 243 nm. The intensities of the positive and negative lobes are approximately equal. This spectrum is characteristic of B-DNA according to Ivanov et al. (1974).

Assignments of Nonexchangeable Protons. In order to determine the structure of the oligonucleotide in more detail, ^1H NMR experiments were carried out. These methods involve first the assignment of the individual protons followed by the determination of the intranucleotide conformations and helical parameters. Finally, molecular dynamics were done to determine if this structure is energetically favorable.

The ^1H NMR spectra were assigned at 293 K using NOESY, TOCSY, and DQF-COSY according to methods described previously (Clore & Gronenborn, 1983; Hare et al., 1983; Patel et al., 1984; Scheek et al., 1983). Assignments are given in Table I. Figure 2A shows a portion of the NOESY spectrum at 200-ms mixing time with the seqential H6/H8 to H1′ assignments. The characteristic internucleotide NOEs for G3H8 to C4H5 and for G17H8 to C18H5 were convenient anchor points for the assignment. The G11H1′ to G11H8 cross-peak is observable only at lower contour levels than shown in Figure 2. The only H6/H8 NOE cross-peak not observed was between G19H8 and G20H1′. None of the resonances for the G20 nucleotide were assigned. The lack of connectivities between these bases may be a result of fraying at the ends or due to degeneracy with a previously assigned resonance. There are a few extra peaks marked by asterisks in the spectrum which reflect the presence of some single-stranded DNA. Figure 2B shows the assignments from the H6/H8 to H2′/H2″ pathway. Sequential NOEs between G5H8 and T6Me, C7H6 and T8Me, and T8H6 and T9Me provide anchor points as well. The only unobserved connectivity in the H6/H8 to H2′/H2″ region was the G3H2′ to C4H6 peak. However,

Table I: Assignment of Nonexchangeable Protons of d(CCGCGTCTTC)·d(GAAGACGCGG) at 293 K[a]

base	H6/H8	Me/H5/H2	H1′	H2′	H2″	H3′	H4′
C1	7.74	5.95	6.01	2.06	2.52	4.73	4.05
C2	7.53	5.68	5.55	2.15	2.44	4.89	4.12
G3	7.89		5.95	2.64	2.72	5.04	4.32
C4	7.29	5.38	5.68	2.05	2.40	4.92	4.15
G5	7.90		6.00	2.65	2.83	5.03	4.35
T6	7.22	1.44	5.63	2.18	2.54	4.94	4.11
C7	7.62	5.62	6.04	2.18	2.54	4.98	4.12
T8	7.46	1.72	5.89	2.18	2.60	4.92	4.21
T9	7.47	1.75	6.20	2.18	2.56	4.85	4.15
C10	7.66	5.88	6.30	2.31	2.21	4.60	4.08
G11	7.96		5.48	2.45	2.72	4.90	
A12	8.22	7.30	5.86	2.65	2.88	5.09	4.42
A13	8.05	7.45	5.95	2.65	2.84	5.07	4.35
G14	7.59		5.52	2.52	2.70	4.98	4.18
A15	8.07	7.60	6.18	2.60	2.85	5.15	4.40
C16	7.15	5.14	5.60	1.94	2.33	4.89	4.11
G17	7.82		5.86	2.60	2.70	4.95	4.23
C18	7.23	5.38	5.64	1.81	2.28	4.89	4.11
G19	7.84		6.18	2.42	2.68	4.90	4.21

[a] Proton assignments at 293 K are based on the connectivities observed in the NOESY, DQF-COSY, and TOCSY spectra (see text). Chemical shifts (in ppm) are referenced to internal DSS. Buffer: 20 mM phosphate, 200 mM KCl, 1.0 mM EDTA, and ^2H_2O, pH 7.2.

this cross-peak is present in the 300-ms NOESY. To assign the H2′/H2″ sugar protons of these nucleotides, the correlations between H1′ in both the TOCSY and NOESY experiments were used (not shown). The NOESY experiment allows unambiguous discrimination between H2′ and H2″ as the H2″ to H1′ NOE always larger than that observed for the H2′ to H1′ NOE. The H3′ and H4′ resonances were assigned from correlations with NOEs observed from H1′ to H3′ and H4′ and from H6/H8 to H3′ and H4′. These were then confirmed with H2′/H2″ to H3′ or H4′ in the TOCSY and from H2′/H2″ to H3′ and from H3′ to H4′ in the DQF-COSY whenever possible. The G11H4′ proton could not be assigned due to signal overlap. The H3′H4′ region of the TOCSY and DQF-COSY is not well resolved and suffers from overlap with the residual HDO peak.

AH2 protons were assigned from cross-strand NOEs as well as NOEs to their imino protons in ^1H_2O (see below). Two AH2 protons had NOEs to each other; thus, they were assigned to either A12 or A13, and subsequently the third AH2 could be assigned to A15H2. A12H2 and A13H2 were distinguished by the presence of a cross-strand NOE between A13H2 and T9H1′ in a 300-ms NOESY.

H6/H8(i) to H6/H8(i+1) NOEs were observed for G3·C4/C4·G5 (peaks are degenerate), G5·T6, T6·C7, A13·G14/G14·A15 (peaks are degenerate), A15·C16, and C18·G19. These cross-peaks indicate that the portion of the DNA from base-pair 3 to base-pair 7 is well stacked in the helix. The presence of an NOE between the T8H6 and T9H6 protons could not be detected because of overlap. C1·G2, C7·T8, T9·C10, A12·A13, A12·G11, and G19·G20 were not observed. These observations may suggest that the bases within the AT-rich region of the duplex are stacked differently into the helix than the bases in the GC-rich region. However, the absence of NOEs in the AT region may be a result of differential relaxation properties within the two regions.

Assignment of Exchangeable Protons. Imino protons were assigned by one-dimensional NOE and two-dimensional NOESY methods in ^1H_2O. These resonances are located between 12.5 and 14.2 ppm (Figure 3), which is typical for imino protons involved in Watson and Crick base-pairings. The imino protons of the terminal nucleotides were assigned

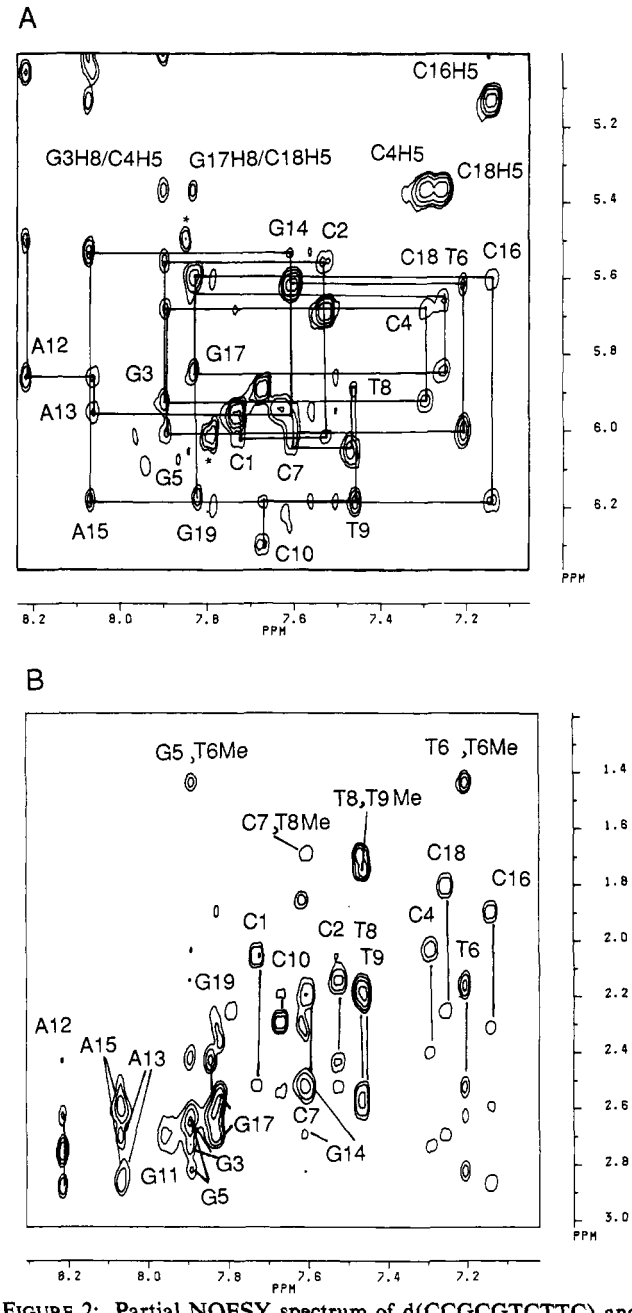

FIGURE 2: Partial NOESY spectrum of d(CCGCGTCTTC) and d(GAAGACGCGG) at 293 K in ^2H_2O. The NOESY spectrum was acquired was acquired and processed as described under Experimental Procedures with a mixing time of 200 ms at 11.7 T. The continuous lines show the sequential assignments (A) H6/H8 to H1′ and (B) H6/H8 to H2′/H2″.

to one of two positions by noting the exchange broadening due to fraying. There was one peak per base-pair for the remaining eight pairs, indicating that the base-pair scheme is symmetric on average. The imino protons of the AT base-pairs were downfield of those observed for the GC base-pairs, as expected. From the 1D NOE experiments, it is clear that the resonance at 12.60 ppm corresponds to CG2 as it only has NOEs to the resonance at 12.86 ppm which corresponds to GC3 and CG4. The AT base-pairs were assigned via the cross-peaks from their imino protons to their AH2s. This left all but two of the resonances assigned. It was difficult to determine which resonance corresponded to base-pair 5 and which to base-pair 7. In the 1D NOE experiments, both of the peaks at 13.01 and 13.22 ppm had NOEs to the AT base-pair at position 6. When AT8/9 was irradiated, it gave a strong NOE to AT6 and weak NOEs to resonances at 13.01 and 13.22 ppm. Both

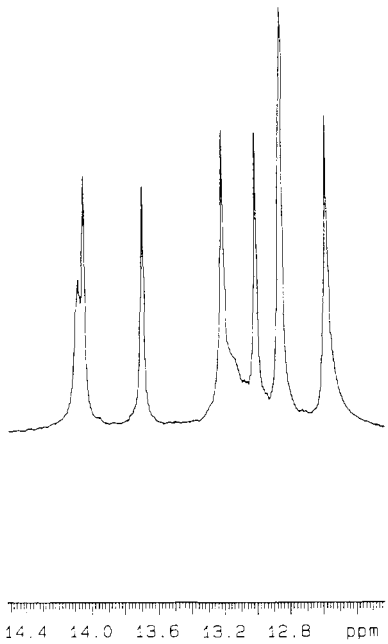

FIGURE 3: 1D ^1H NMR spectrum of the imino proton region in ^1H_2O at 293 K. The spectrum was recorded as described under Experimental Procedures.

of these peaks were affected even at short irradiation times. This indicates that the base stacking in the helix must allow for efficient spin diffusion. Unfortunately, it makes it impossible to know which resonance, the one at 13.01 ppm or the one at 13.22 ppm, corresponds to position 5 or to position 7. Chemical shift values are reported in Table II.

Calculation of Correlation Times and Selective T_1's. The apparent correlation time τ_c was determined for all of the C(H5–H6) vectors which occur in this sequence according to the method of Lane et al. (1986). The average τ_c determined from the internal cytosines is 3.2 ns which is near that expected for a 10-mer at 20 °C. The terminal cytosines C1 and C10 had shorter τ_c's than the internal cytosines presumably because of fraying effects. C7 was not included in the calculation because the C7H5 peak overlapped with the T6H1′ peak.

Selective T_1 experiments were also carried out on C16, A12, and A13/A15 base protons. These protons were chosen because they are the only well-resolved peaks in a 1D spectrum of the base region. These values were 290 ms (C16H6), 280 ms (A12H8), and 230 ms (A13/A15H8). These T_1 values are in agreement with what one expects given the average τ_c of 3.2 ns for B-DNA. The T_1 values were used for the normalization of NOEs to zero mixing time as described under Experimental Procedures.

Nucleotide Conformation. Qualitatively, all bases are in the anti orientation as seen by the relative NOE intensities: H8/H6 to H2′ > H2″ > H1′. Specifically, the H8/H6 to H1′ NOEs are very weak as one expects for the anti orientation. Precise glycosidic torsion angles were calculated for many of the bases by analyzing NOE time courses using the NUCFIT program (Lane, 1990) as described under Experimental Procedures. In order to calculate accurate glycosidic torsion angles, bases need to have well-resolved sugar proton resonances. The NOE which is most sensitive to the glycosidic torsion angle is that between H2′ and H6/H8. Unfortunately, only some of the bases have sugar resonances that meet this criterion: C1, C2, C4, T6, C10, C16, and C18. All of these nucleotides have calculated glycosidic torsion angles of ca.–110° from NUCFIT, which is characteristic of B-DNA and not −150° which is characteristic of A-DNA. Values are reported in Table III.

Table II: Assignment of the Imino Protons of d(CCGCGTCTTC)·d(GAAGACGCGG)[a]

base-pair	chemical shift (ppm)	base-pair	chemical shift (ppm)
C1·G20	13.10/12.54	T6·A15	13.72
C2·G19	12.60	C7·G14	13.01/13.22
G3·C18	12.86	T8·A13	14.00
C4·G17	12.86	T9·A12	14.10
G5·C16	13.01/13.22	C10·G11	13.10/12.56

[a] The assignments were obtained from 1D NOE and NOESY experiments in ^1H_2O (see text). Chemical shifts were referenced to internal DSS. Buffer: 20 mM sodium phosphate, 200 mM KCl, 1.0 mM EDTA, and 10% ^2H_2O at pH 7.0.

Table III: Glycosidic Torsion Angles and Pseudorotation Angles[a]

base	χ[d]	P[d]	f_S[e]	$\Sigma 1'$[f]	$\Sigma 2'$[f]
C1	−105	30–45	10–55	11.1 ± 1.9	23.0 ± 4.4
C2	−115	35–90	45–85	14.6 ± 2.2	27.8 ± 6.2
G3	(−110)[b]	30–40	15–50	11.5 ± 1.0	26.0[c]
C4	−110	30–40	15–50	11.5 ± 1.0	23.0 ± 4.5
G5	−110	40–90	50–85	14.1 ± 1.3	27.5 ± 2.8
T6	−110	30–65	30–85	12[c]	nd[b]
C7	(−110)[b]	45–80	65–85	14.7 ± 1.3	24.1 ± 1.0
T8	−95	30–50	30–70	12.4[c]	24.0[c]
T9	(−110)[b]	30–50	25–60	12.3 ± 1.1	26.3 ± 1.9
C10	−80	30–45	20–55	12.0 ± 1.0	nd[b]
G11	(−110)[b]	30–50	20–55	12.1 ± 1.0	nd[b]
A12	−125	30–50	10–55	11.6 ± 1.5	nd[b]
A13	−100	35–55	40–70	13.0 ± 1.0	24.9 ± 1.9
G14	−130	40–60	50–80	13.6 ± 1.0	nd[b]
A15	(−110)[b]	30–45	20–50	11.9 ± 1.0	23.0[c]
C16	−105	35–50	20–60	12.1 ± 1.4	25.4 ± 2.3
G17	−125	45–90	55–100	14.3 ± 1.4	28.7 ± 1.0
C18	−115	30–50	10–45	11.7 ± 1.9	26.7 ± 5.5
G19	(−110)[b]	30–40	10–45	11.4 ± 1.0	27.0 ± 5.7

[a] Coupling constants were determined from NOESY, TOCSY, and DQF-COSY. Means and standard deviations were calculated from coupling constants obtained from these three experiments when possible (see text). The range of pseudorotation angles was calculated according to Rinkel and Altona (1987). Glycosidic torsion angles were determined using NOESY cross-peak intensity as described in the text. [b] Not all cross-peaks were observed due to overlap: see text. nd, not determined. [c] From single measurement only so no standard deviation is reported. The ranges of f_S and P_S in these cases are calculated assuming $\Sigma 1'$ is only determined to within 1 Hz. [d] Glycosidic torsion angles and pseudorotation angles in degrees. Values have been rounded to the nearest 5°. Ranges were determined as described in the text. [e] The fraction south multiplied by 100. [f] $\Sigma 1'$ and $\Sigma 2'$ are in hertz.

Most of the H2′/H2″ base region in the NOESY is plagued by overlap particularly from internucleotide NOEs. (Thus, these resonances can still be assigned and pseudorotation angles determined using through-bond experiments.) The H8/H6 to H2′ cross-peak overlaps with other cross-peaks in the NOESY so that only a maximum volume can be determined. In such cases, the value calculated for the glycosidic torsion angles will be systematically smaller, e.g., more syn-like than the real value. The glycosidic torsion angles determined in this way are also given in Table III. Some glycosidic torsion angles could not be determined because of overlap problems. However, the NOE pattern (small H8/H6 to H1′ and large H8/H6 to H2′ NOEs) indicated that these were in an anti orientation. These were given a value of −110°.

Sugar Pucker Conformation. For energetic reasons, deoxyfuranose rings are not planar but must have at least one atom outside the plane of the ring. The mode and degree as to which this is accomplished are referred to as sugar puckering [see review by Saenger (1984) and Rinkel and Altona (1987)]. Two energetically favored sugar puckers are C3′-endo (north) and C2′-endo (south). The sugar pucker can be considered

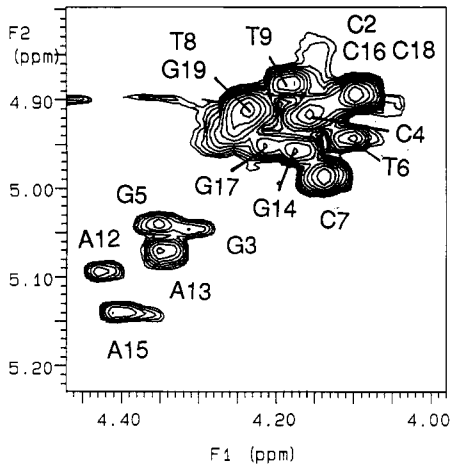

FIGURE 4: Partial TOCSY spectrum showing a portion of the H3′H4′ region at 293 K in ^2H_2O. The TOCSY spectrum was acquired and processed as described under Experimental Procedures with a mixing time of 50 ms at 14.1 T.

as a unique conformation which is defined by the value of the pseudorotation angle. Rinkel and Altona (1987) have calculated the values for coupling constants and sums of coupling constants consistent with a given pseudorotation angle (P). However, they have also shown that the coupling constant data are not always consistent with a single sugar pucker. In the absence of a complete set of coupling constants, it is possible to model the sugar conformation either as a unique conformation or as a mixture of states. First, the simpler case of the unique conformation will be considered. It is important to note that values of pseudorotation angles are inherently imprecise because thermal motions alone cause perturbations of the sugar pucker of ~30° (Swaminathan et al., 1991). Further, if one determines the value of the pseudorotation angle from coupling constants by the method of Rinkel and Altona (1987), the precision for such measurements is usually reported as 1 Hz. The precision of these measurements is commonly limited by the digitization of the data. However, this indicates that the pseudorotation value is only determined to within ~20°. In this report, the digitization is 0.73 Hz/point, and thus coupling constants cannot be determined with much greater accuracy than that. For these reasons, pseudorotation angles (P) are considered as ranges of values and not as single values.

Qualitatively, the presence or absence of cross-peaks can be used to determine a range of pseudorotation angles consistent with the data (Hosur et al., 1986). Coupling constants particularly sensitive to values of P are H1′H2′, H2″H3′, and H3′H4′. The presence of an H1′H2′ cross-peak in the TOCSY or DQF-COSY indicates that $P \geq 30°$ and $P \leq 240°$. In the case of the protons from T6 and T8, the H1′2′ cross-peak was very weak. Thus, these cross-peaks have a $P \sim 30°$. Because of overlap, the presence/absence of H1′H2 peaks corresponding to G11 and G14 cannot be ascertained. However, the remaining nucleotides have substantial $^3J_{1'2'}$, suggesting $P > 30°$. Further, the presence of H2″ to H3′ cross-peaks eliminates pseudorotation angles above 90° and below 250°. Finally, the cross-peaks betwen H3′ and H4′ sugar protons in the DQF-COSY and TOCSY indicate that $P \leq 130°$ or $P \geq 300°$. Part of the H3′4′ region of the TOCSY is shown in Figure 4. From the above coupling constant data, the approximate range of the pseudorotation angle for most nucleotides is $30° < P < 90°$. The absence of the H2″H3′ cross-peak for A13, G14, and G17 indicates that the range for these nucleotides is $90° < P < 130°$.

Analysis of cross-peak fine structure was used to determine a more precise value of P. The pseudorotation angles were determined as described by Rinkel and Altona (1987) and are reported in Table III. The $\Sigma 1'$ and $\Sigma 2'$ coupling constants were measured in NOESY, TOCSY, and DQF-COSY spectra when possible. Standard deviations are calculated for each set of $\Sigma 1'$ and $\Sigma 2'$ values obtained from more than one spectrum. However, in some cases, these data could only be obtained by one or two of the above experiments due to spectral overlap. This was a problem especially in the NOESY where intranucleotide NOEs are present. By obtaining the coupling constants from both anti-phase and in-phase experiments, errors from measuring the apparent separation rather than the true separation can be minimized. The ranges of pseudorotation angles are determined as described above. The qualitative data obtained above are used as constraints when there is more than one value of P which is consistent with the values for $\Sigma 1'$ and $\Sigma 2'$. For instance, pseudorotation angles of 200° and of 65° are both consistent with the $\Sigma 1'$ data for G5. The 200° value can be ruled out because the G5 nucleotide has a H3′H4′ cross-peak in the TOCSY which indicates that $P \leq 130°$. The important fact to note is that none of these sugar puckers appears to be in a standard C2′-endo conformation. Most of the sugar puckers appear to be more north-like than south-like. There appears to be some contradiction between the range of P calculated for A13, G14, and G17 based on the absence of H2″H3′ cross-peaks and the values calculated for P from the $\Sigma 1'$ data. This suggests that there may be exchange between sugar conformations of these nucleotides.

NOE data were also analyzed to resolve any ambiguities in the determination of the value of P. Many of the $\Sigma 1'$ and $\Sigma 2'$ values were consistent with more than one range of pseudorotation angles: C3′-endo/C4′-exo/O1′-endo and O4′-exo/C4′-endo. However, values for a unique range of P were selected on the basis that only C3′-endo/C4′-exo was consistent with the NOE data in the H1′ to H4′, H2″ to H4′, and H6/H8 to H4′/H5′/H5″ regions. From simulations using NUCFIT on the O4′-exo/C4′-endo ($P \sim 250°$) conformations, one expects the NOEs between the H6/H8 protons of the nucleotide and the H5′/H5″ protons of the sugar to be larger in magnitude than any other intranucleotide NOE. For the nucleotides observed here, the H5′/H5″ to H6/H8 NOEs were smaller than the NOEs between H1′ and H6/H8. (Although the H5′/H5″ protons were not assigned to individual nucleotides because of spectral overlap, resonances in the correct spectral region could be assigned to being H5′/H5″ protons). Therefore, values of $P \sim 250°$ could be ruled out. For all nucleotides with definitive assignments of H4′, cross-peaks are also observed between H2″ and H4′ in the NOESY. According to van de Ven and Hilbers (1988), these NOEs are observed when $0° < P < 100°$. Again, this is consistent with the other data.

Of course, it is also possible that the sugars exist as a mixture of sugar puckers rather than as a unique range of conformations. Exchange between north and south sugar puckers is known to occur on the nanosecond time scale (Porschke, 1978). Since the energy barrier between sugar conformations in the region $0° < P < 200°$ is low, it is reasonable to expect that the sugar rings may exist in several conformations. For example, Schmitz et al. (1990) report that the conformation of the sugar rings in their 8-mer can be described by exchange between two or three states. Rinkel and Altona (1987) have shown that the value of $\Sigma 1'$ can be used to determine the f_S because there is less than 1-Hz variation in the values of $\Sigma 1'$

at a given value of P_S for values between 80° and 200°. As with the unique conformation, certain quantitative conclusions regarding f_S can be deduced simply by the presence/absence of the H1′H2′, H2″H3′, and H3′H4′ cross-peaks. Simulations using NUCFIT have been carried out using values varying from 80° to 200° for P_S and 9° for P_N to determine values for coupling constants. From these calculations, it is clear that the presence of H1′H2′ cross-peaks indicates that $f_S >$ 10% and the presence of H3′H4′ cross-peaks suggests that f_S < 85%. Further, the presence of H2″H3′ cross-peak indicates f_S < 70%. One should note that the values of $J_{3'4'}$ and $J_{2''3'}$ are more dependent on the value of P_S used in the simulation than the $\Sigma 1'$ value is. Thus, the values of f_S obtained from observing the presence of H2″H3′, H3′H4′ cross-peaks are only approximate. In order to determine a more precise value of f_S, one can use the $\Sigma 1'$ value obtained above and calculate f_S as described by Rinkel and Altona (1987). Once again, limitations of determining the value of $\Sigma 1'$ to only 1 Hz mean that the value of f_S can only be determined to within 20%. For this reason, values of f_S are given in ranges. Values are reported in Table III. Ranges are calculated using the standard deviation of the $\Sigma 1'$ values and the method of Rinkel and Altona (1987). One can see that the value of f_S is poorly determined. Nevertheless, it is clear that many sugars exist in a north-like sugar pucker which is more commonly observed in A-DNA than in B-DNA.

The possibility of exchange between double- and single-stranded forms of the DNA can be eliminated since the H8/H6 to H1′ cross-peaks are not unusally broad. Further, any exchange on the chemical shift time scale can be ruled out since no ROESY peaks were observed at mixing times of 75, 100, and 200 ms.

Determination of Helical Parameters. From the pattern of intranucleotide and internucleotide NOEs, it is clear that this oligonucleotide is a right-handed helix and that the overall conformation is B-like rather than A-like. This result is consistent with the CD data (see above). The expected NOE pattern for the H6/H8(i) to sugar protons(i) was calcualted using the NUCFIT program for several values of P and χ. The pattern of NOE intensities for the individual nucleotide H6/H8 protons to the sugar protons observed experimentally in the 200-ms NOESY is H2′ > H2″ > H1′ > H3′,H4′,-H5′,H5″ in general (see Figure 5A,B,C). For A-DNA, with P = 10° and χ = −150°, the following helical parameters were used: twist of 32.7°; 0.29 nm for rise; base roll of 0°; tilt of 20°; and shift of −0.4 nm. The patterns of the intensity for a 200-ms NOESY from the H6/H8 protons were calculated to be H5″ > H3′ > H2′ > H4′ ~ H1′ > H2″. Figure 5 clearly indicates that this is not the pattern observed for the nucleotides of the ATF binding site.

Similar calculations were carried out to determine the relative magnitude of the NOEs between the H6/H8(i) and sugar(i) protons for B-DNA where P = 162° and χ = −110°. For standard B-DNA conformations, NUCFIT assumes the following helical parameters: twist of 36°; rise of 0.34 nm; base-pair roll of 0°; tilt of 0°; and shift of 0.02 nm. The pattern of NOE intensities calculated was H2′ > H2″ > H5″ > H1′ ~ H3′ > H4′ > H5′. Simulations were also completed using a B*-form which was as B-DNA except that propeller twists were nonzero and the glycosidic torsion angles were set to −100° for purines and −120° for pyrimidines. The relative intensities obtained for this case were H2′ > H2″ > H3′ > H1′ > H5″ > H5′ > H4′. The relative intensities of internucleotide NOEs also show that the DNA has B-like features. The base(i) to H2″(i−1) is more intense than the base(i) to H2′(i−1) (Figure 5). In A-DNA, one expects the reverse trend. Although the NOE pattern observed for the ATF oligonucleotide is more like the B- and B*-DNAs than the A-DNA, it clearly has different nucleotide conformations than one would expect for either of these forms.

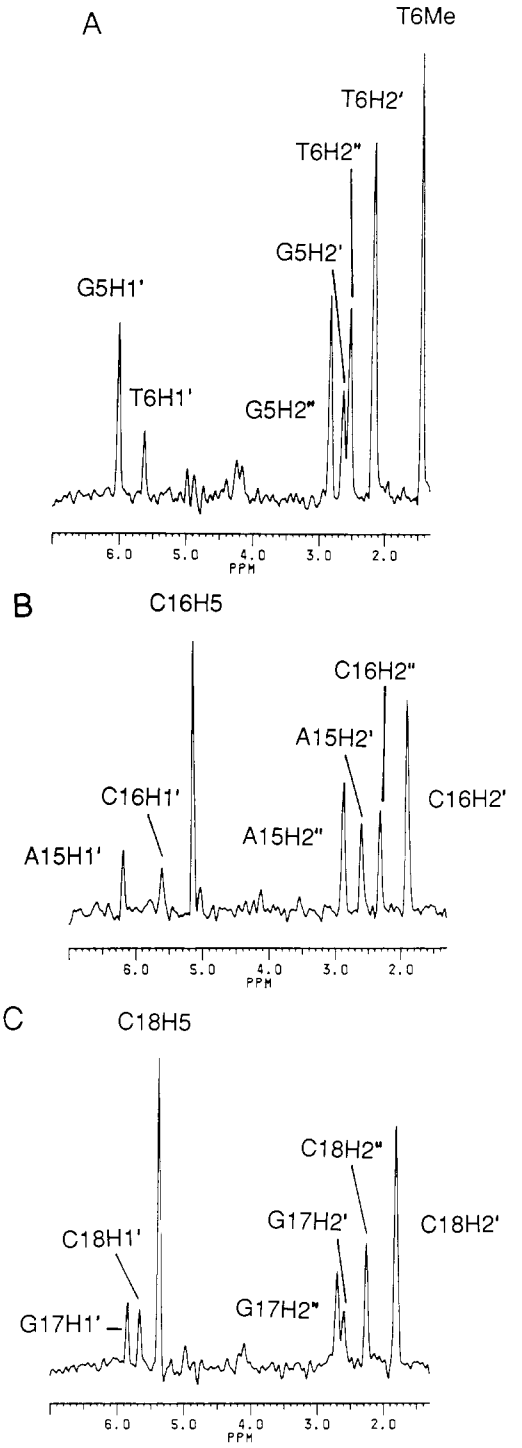

FIGURE 5: Cross sections through H6/H8(i) protons to sugar protons-(i,i−1) from a NOESY spectrum (200 ms) in ^2H_2O at 293 K. Sequential and intranucleotide connectivities are shown for rows through T6H6 (A), C16H6 (B), and C18H6 (C). The cross sections are scaled identically. See Experimental Procedures for details of the data collection and processing.

Helical parameters were calculated in order to obtain more information on the structure of the DNA. These calculations were carried out in order to determine what general type of helix was consistent with the data. NOE time courses were used as input into NUCFIT in order to determine the ranges of the helical parameters. The cross-peaks of interest here

Table IV: Helical Parameters Determined from the NOE Time Course Data and the Program NUCFIT[a]

base	twist[b]	rise[c]	tilt[b]	shift[c]	roll[b]	*R*
C2·G19						
G3·C18	36/40	0.31/0.35	0/−5	0/0.1	10,10/30,30	0.29/0.34
G3·C18						
C4·G17	32/40	0.34/0.32	0/−1	0/−0.05	0,0/20,20	0.20/0.25
C4·G17	32/36	0.41/0.43	0/−1	0/−0.1	10,10/20,20	0.39/0.42
G5·C16						
G5·C16						
T6·A15	32/38	0.37/0.42	0/−1	0/−0.1	10,10	0.24/0.26
T9·A12	34/38	0.34/0.40	0/−1	0/−0.1	0,0/20,20	0.16/0.20
C10·G11						

[a] *R* is the mean average fractional deviation as calculated by NUCFIT. See Experimental Procedures for details of analysis. Where appropriate, a range of values for each helical parameter giving similar fits is reported. The corresponding range of *R* is also given. [b] Values are in degrees. [c] Values are in nanometers.

are the H8/H6(*i*) to H1′/H2′/H2″(*i*−1). The NOE cross-peak volume data could only be used to calculate the helical parameters for five dinucleotide pairs. This is because the large degree of spectral overlap in the NOESY, especially of the H2′ and H2″ resonances, prevented calculation of many cross-peak volumes. Fortunately, most cross-peaks are well enough resolved that one can see that H2″ > H2′. However, these peaks are not resolved enough to determine accurate cross-peak volumes. Some of the resonances are nearly degenerate, e.g., T8 and T9. Thus, only qualitative conclusions for the remainder of the oligonucleotide can be made.

The following steps were fit using NUCFIT: C2G3/C18G19, G3C4/G17C18, C4G5/C16G17, G5T6/A15C16, and T9C10/G11A12. Not surprisingly, most of these steps have alternating purine/pyrimidine bases. In general, such sequences give better resolved data. For the purpose of the fitting, all *P* values were considered to be a unique conformation as determined from the coupling constants and not a mixture of states. However, this unique conformation should be thought of as an average state within the range given, not one frozen conformation.

Of the helical parameters (rise, twist, roll, tilt, and shift) determined using NUCFIT, the base roll (and therefore propeller twist) is the least dependent on internucleotide H1′, H2′, and H2″ to H6/H8 NOEs and therefore cannot be well determined, i.e., not better than 10° (Lane, 1990). Some base steps have large shifts. There appear to be large propeller twists for all the dinucleotide pairs studied. The helical parameters are typical for B-DNA. Ranges of the helical parameters twist, rise, roll, and shift which were calculated using NUCFIT are given in Table IV. The values within these ranges had similar values for the fits. One problem with fitting the data in this manner is that many of the parameters are covariant. This inevitably leads to large ranges on these parameters. One should not that although these values are consistent with the data, they are not necessarily the only set of parameters which fit the data. However, the CD data clearly indicate that the helix is in a B-like conformation. It is clear that these data are not consistent with an A-like conformation.

Energy Minimization and Molecular Dynamics. Molecular dynamics calculations were carried out simply to determine whether the B-like helix with C3′-endo/C4′-exo/O1′-endo sugar puckers and anti-glycosidic torsion angles is an energetically favorable conformation. The glycosidic torsion angles and pseudorotation angles were set to those determined by the NMR data and were entered as constraints (see Experimental Procedures). Large negative energies were obtained from the calculations under these conditions, indicating that such a structure is energetically feasible. The calculated structures also resulted in structures with large propeller twists and typical values for B-helical conformations.

This work agrees with previous reports which suggest that not all oligonucleotide structures fall into well-defined categories seen in the crystalline state. The conformation of the ATF binding site shows that even with alterations in the phosphodiester backbone as a result of the C3′-endo/C4′-exo/O1′-endo sugar conformations the helix can still exist in a B-like form. Clearly, it is not present in the archetypal B-form but in a conformation close to it. Unfortunately, because of the severe overlap problems in the NOESY spectra and the limitation of the method itself, a unique family of structures cannot be determined for this sequence. At this stage, it is impossible to determine whether this conformation is a property of viral DNA, ATF binding sites in general, or this sequence in particular.

ACKNOWLEDGMENT

Thanks to B. Peck for assistance with DNA purification and S. Martin for assistance with CD studies. I am also grateful for critical discussions of the manuscript with A. Lane.

REFERENCES

Aboula-ela, F., Varani, G., Walker, G. T., & Tinoco, I. (1988) *Nucleic Acids Res. 16*, 3559–3572.

Altona, C., & Sundaralingam, M. (1972) *J. Am. Chem. Soc. 94*, 8205–8212.

Bauer, C. J., Frenkiel, T. A., & Lane, A. N. (1990) *J. Magn. Reson. 87*, 144–152.

Bax, A., & Davis, D. G. (1985) *J. Magn. Reson. 65*, 355–360.

Bax, A., & Lerner, L. (1988) *J. Magn. Reson. 79*, 429–438.

Borden, K. L. B., Jenkins, T. C., Skelly, J. V., Brown, T., & Lane, A. N. (1992) *Biochemistry 31*, 5411–5422.

Bothner-By, A. A., Stevens, R. L., Lee, J. T., Warren, C. D., & Jeonloz, R. W. (1984) *J. Am. Chem. Soc. 106*, 811–815.

Carbonnaux, C., van der Marel, G. A., van Boom, J. H., Guschlbauer, W., & Fazakerly, G. V. (1991) *Biochemistry 30*, 5449–5458.

Chary, K. V., Hosur, R. V., Govil, G., Chen, C., & Miles, H. T. (1988) *Biochemistry 27*, 3858–3867.

Chou, S.-H., Flynn, P., & Reid, B. (1989) *Biochemistry 28*, 2435–2443.

Clore, G. M., & Gronenborn, A. M. (1983) *EMBO J. 2*, 2109–2115.

Fairall, L., Martin, S., & Rhodes, D. (1989) *EMBO J. 8*, 1809–1817.

Freemont, P. S., Lane, A. N., & Sanderson, M. R. (1991) *Biochem. J. 278*, 1–23.

Frenkiel, T. A., Bauer, C. J., Carr, M. D., Birdsall, B. B., & Feeney, J. (1990) *J. Magn. Reson. 90*, 420–425.

Gao, X., & Patel, D. J. (1988) *J. Am. Chem. Soc. 110*, 5178–5182.

Hai, T., Liu, F., Coukos, W. J., & Green, M. R. (1989) *Genes Dev. 3*, 2083–2090.

Hare, D. R., Wemmer, D. E., Chou, S.-H., Drobny, G., & Reid, B. R. (1983) *J. Mol. Biol. 171*, 319–336.

Hore, P. J. (1983) *J. Magn. Reson. 55*, 283–300.

Hosur, R. V., Ravikumar, M., Chary, K. V. R., Sheth, A., Govil, G., Zo-Kun, T., & Miles, H. T. (1986) *FEBS Lett. 205*, 17–76.

Ivanov, V. I., Minchenkova, L. E., Minyat, E. E., Frank-Kanenetskii, M. D., & Scholkina, A. K. (1974) *J. Mol. Biol. 87*, 817–833.

Kim, S.-G., & Reid, B. R. (1992) *Biochemistry 31*, 12103–12116.
Lane, A. N. (1989) *Mol. Cell. Biol. 8*, 53–61.
Lane, A. N. (1990) *Biochim. Biophys. Acta 1049*, 189–204.
Lane, A. N. (1991) *Carbohydr. Res. 221*, 123–144.
Lane, A. N., & Forster, M. J. (1989) *Eur. Biophys. J. 17*, 221–232.
Lane, A. N., Lefevre, J.-F., & Jardetzky, O. (1986) *J. Magn. Reson. 66*, 201–218.
Lane, A. N., Jenkins, T. C., Brown, D. J. S., & Brown, T. (1991) *Biochem. J. 279*, 269–281.
Lauble, H., Frank, R., Blocker, H., & Heinemann, U. (1988) *Nucleic Acids Res. 16*, 7799–7816.
Leonard, G. A., Booth, E. D., & Brown, T. (1990) *Nucleic Acids Res. 18*, 5617–5623.
Li, Y., Zon, G., & Wilson, W. D. (1991) *Proc. Natl. Acad. Sci. U.S.A. 88*, 26–30.
Marion, D., & Wuthrich, K. (1983) *Biochem. Biophys. Res. Commun. 124*, 774–783.
McCall, M., Brown, T., Hunter, W. N., & Kennard, O. (1986) *Nature 322*, 661–664.
Mirau, P. (1988) *J. Magn. Reson. 80*, 439–447.
Patel, D. J., Kozlowski, S. A., Ikuta, S., & Itakura, K. (1984) *Biochemistry 23*, 3207–3217.
Porschke, D. (1978) *Biopolymers 17*, 315–323.
Rajagopal, P., Gilbert, D. E., van der Marel, G. A., Boom, J. H., & Feigon, J. (1988) *J. Magn. Reson. 78*, 526–537.
Rinkel, L. J., & Altona, C. (1987) *J. Biomol. Struct. Dyn. 4*, 621–649.
Rinkel, L. J., van der Marel, G. A., van Boom, J. H., & Altona, C. (1987) *Eur. J. Biochem. 166*, 87–101.
Saenger, W. (1984) *The Principles of Nucleic Acids*, Springer-Verlag, New York.
Scheek, R. M., Russo, N., Boelens, R., & Kaptein, R. (1983) *J. Am. Chem. Soc. 105*, 2914–2916.
Schmitz, U., Zon, G., & James, T. L. (1990) *Biochemistry 29*, 2357–2368.
States, D. J., Haberkorn, R. A., & Ruben, D. J. (1982) *J. Magn. Reson. 48*, 286–292.
Steitz, T. A. (1990) *Q. Rev. Biophys. 23*, 205–280.
Swaminathan, S., Ravishanker, G., & Beveridge, D. L. (1991) *J. Am. Chem. Soc. 113*, 5027–5041.
Tassios, P. T., & LaThangue, N. B. (1990) *New Biol. 2*, 1123–1134.
van de Ven, F. J., & Hilbers, C. W. (1988) *Eur. J. Biochem. 178*, 1–38.
van Wijk, J., Huckriede, B. D., Ippel, J. H., & Altona, C. (1992) *Methods Enzymol. 211*, 286–306.
Wagner, G., & Wuthrich, K. (1979) *J. Magn. Reson. 33*, 675–680.